# بررسی جفت‌شدگی مد پلاسمونی در دو نانونوار طلا

محمدرضا حسن پور و مصطفی قربان‌زاده

دانشگاه حکیم سبزواری، دانشکده مهندسی برق و کامپیوتر، سبزوار

چکیده- در این مقاله، با استفاده از جفت‌شدگی دو نانونوار طلا، یک بستر جدیدی را برای تشخیص و تله‌اندازی نانوذرات پیشنهاد می‌دهیم که از پلاسمون‌های سطحی انتشاری تحصیر و تقویت شده با نیم‌رخ مد متفاوت بهره می‌برد.ما با استفاده از روش تفاضل محدود مد ویژه (FDE) به بررسی مدهای پلاسمونی که مابین دو نوار طلا جفت شده تحریک می شوند، می‌پردازیم. ما در این بررسی نشان می‌دهیم که در ساختار فلز-دی الکتریک-فلز ارائه شده، پروفایل مدهای پلاسمونی، ضریب شکست موثر و میزان تلفات، وابستگی زیادی به ماده تشکیل دهنده عایق (محیط حس‌کنندگی)، ابعاد ساختار و فرکانس تابشی منبع دارد.

کلید واژه- پلاسمون‌های سطحی، تلفات، جفت‌شدگی موجبر، سنسور نوری، ضریب شکست موثر.

## Investigation of plasmonic mode Coupling of two Gold Nano-strips

### Mohammad-reza Hasanpour and Mostafa Ghorbanzadeh

### Faculty of Electrical and Computer Engineering, Hakim Sabzevari University, P.O. Box 397, Sabzevar 9617976487, Iran.

### m.ghorbanzadeh@hsu.ac.ir

Abstract- In this paper, by coupling two gold strips we propose a new platform for sensing and trapping nanoparticles that benefit from enhanced and confined propagating surface plasmons with different mode profiles. We study the plasmonic modes that can be excited between these two coupled gold strips by the Finite difference eigenmode (FDE) method. We show that, in this Metal-Insulator-Metal (MIM) structure, the plasmonic mode profiles, effective refractive index ($n_{eff}$), and loss factor, strongly depend on insulator material (or sensing medium), the dimension of the structure, and the illuminated source frequency.

Keywords: Effective refractive index, loss, opto-sensor, surface plasmons, waveguide coupling.

The ۲۸th Iranian Conference on Optics and Photonics (ICOP ۲۰۲۲)
The ۱٤th Iranian Conference on Photonics Engineering and Technology (ICPET ۲۰۲۲)
Shahid ChamranUniversity of Ahvaz, Khuzestan, Iran, Feb. ۱-۳, ۲۰۲۲.

## ۱. Introduction

Plasmons are the collective motion of free electrons in metals coupled with light that makes a variety of applications at the nano-scale range [۱]. Excitation of plasmons for a metal such as gold (Au) can be realized by the momentum matching technique to create a localized and enhanced field at the visible range of the light spectrum [۲]. Due to subwavelength waveguiding, light concentration beyond the diffraction limit, ultrafast response, high environmental sensitivity and, flexibility in design, surface plasmons attract more attention in developing different types of sensors [۳] and especially optical tweezers for example based on the propagating surface plasmons on top of a single gold strip layer [٤].

In this paper, by coupling two gold strips we propose a new platform for sensing and trapping nanoparticles that benefit from enhanced and confined propagating surface plasmons with different mode profiles. We study the plasmonic modes that can be excited between two coupled gold strips by the finite difference eigenmode (FDE) method. We show that, in this Metal-Insulator-Metal (MIM) structure, the plasmonic mode profiles, effective refractive index ($n_{eff}$), and loss factor, strongly depend on insulator material (or sensing medium), the dimension of the structure, and the illuminated source frequency.
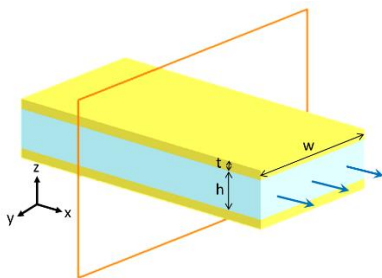
## ۲. Structure and simulation method



Fig. ۱: The structure of coupled Gold strip

The coupled gold strip waveguide is made up of three main parts including a middle dielectric layer and top and bottom gold (Au) metal layers that are shown in Fig .۱. The height of the middle dielectric layer, the thickness of the metal layer, and the width of the waveguide are indicated by $h$ and $t$, and $w$, respectively. The frequency of the source (that will be injected along the $-x$ direction) is set to ۳٦۰ THz (~۸۳۳ nm), which is compatible with biological objects.

In Fig. ۲(c) the $y$-$z$ cross-section of the waveguide is illustrated. Here, the selected values for the dimensions are ۵۰ nm, ۲۰۰ nm and, ۵۰۰ nm for $t$, $h$, and $w$, respectively. In these simulations, we have only considered the first five modes which had the highest $n_{eff}$. In Fig .۲(a)-(b), the vertical yellow line at the $h$=۲۰۰ nm shows the effective index and loss factor of the waveguide by the mentioned $h$,$w$ and, $t$ values. the profile of the electric fields in both $x$ and $z$ directions ($\mathbf{E}_x$ and $\mathbf{E}_z$), the real part, and the phase of the mentioned fields have been analyzed to distinguish and label them.
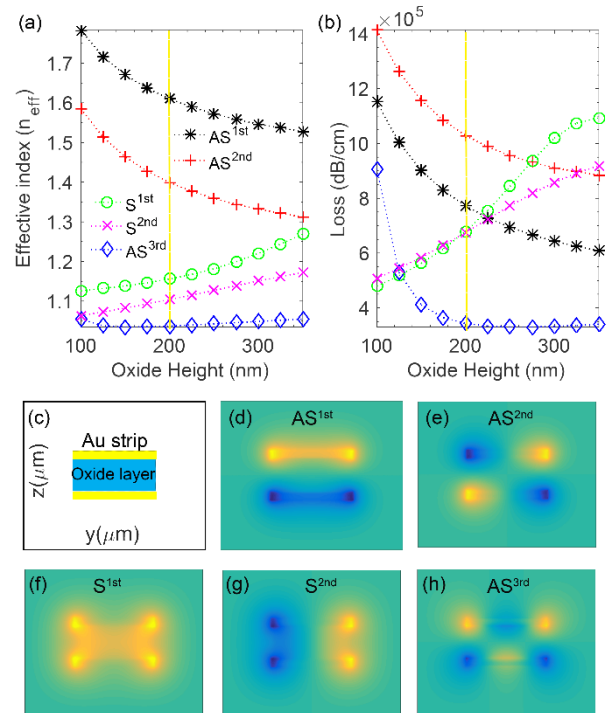


Fig. ۲: (a)-(b) Effective refractive index and loss variations with varied dielectric height $h$. (c) Cross-section view of MIM waveguide at the $y$-$z$ plane. (d)-(h) $E$ profiles of MIM waveguide at the $y$-$z$ plane. $w$= ۵۰۰ nm, $h$=۲۰۰ nm and $t$=۵۰ nm

The ۲۸th Iranian Conference on Optics and Photonics (ICOP ۲۰۲۲)
The ۱٤th Iranian Conference on Photonics Engineering and Technology (ICPET ۲۰۲۲)
Shahid ChamranUniversity of Ahvaz, Khuzestan, Iran, Feb. ۱-۳, ۲۰۲۲.

## ۳. Simulation and Results

The observed modes have been categorized based on the symmetry of the electric field respect to the *y* axis at the middle of the dielectric layer, in the *y-z* plane. Fig. ۲(d)-(h) respectively shows the AS$^{1st}$, AS$^{2nd}$, AS$^{3rd}$, S$^{1st}$, and S$^{2nd}$ modes in which S and AS represent the Symmetric and the Anti-symmetric modes and the superscript indicates the mode number. In the following sections the effect of waveguide dimensions, frequency, and insulating refractive index have been investigated.

### ۳,۱ □□□□□□□□ □□□ □□□□□ □□□□□ □□□□□□□□

In Fig .۲(a)-(b) we swept the height of the dielectric *h* between ۱۰۰:۳٥۰ nm with ۲٥nm steps meanwhile, the thickness of the Au layer *t* and the width of the structure *w* is remained constant at ٥۰nm and ٥۰۰□□, □□□□□□□□□□□. □□□ □□ □□□□ □□□□□□□□□ □□□□□□□□ □□ *h*, the type of the modes may differ. According to the simulations, the modes with higher $n_{eff}$ (AS$^{1st}$) still can belong to the same category for a wider interval. The intervals we have selected in the figures are the maximum common valid range from the aspect of categorization. Hence, some of the modes may continue for a limited interval of the sweeping parameter.

According to Fig. ۲(b), it's noticeable that by increasing the oxide height *h* for the interval between ۱۰۰ and ۳٥۰ nm, the loss factor of the anti-symmetric modes decreases exponentially. In contrast, the loss factor of symmetric modes increase uniformly.

### ۳,۲ □□□□□□□□ □□□ □□□□□ □□ □□□ □□□□□□□□□

Fig. ۳ (a)-(b) demonstrates the variations of the $n_{eff}$ and *loss* versus the structure width *w*. Referring to Fig. ۳ (a), AS$^{1st}$ has the highest $n_{eff}$ among all other modes. All three anti-symmetric modes showed significant growth while widing the structure. However, the symmetric are converging to the value of $n_{eff}$=۱,۱. In the given range of *w*, the $n_{eff}$ of the AS$^{1st}$, AS$^{2nd}$, and AS$^{3rd}$ increase ۰,۰٤, ۰,٤۲, and ۰,۳۷, □□□□□□□□□□□. □□□ . ۳(b) □□□□□□□□□□ □□□ □□□□□□□□□

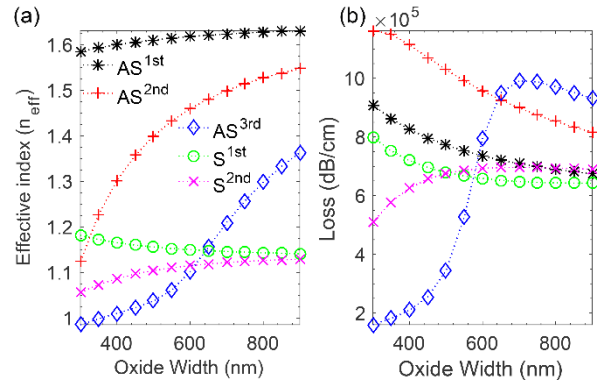of the loss of the waveguide. In this graph, the AS$^{3rd}$ has the highest variation relative to all other modes.



Fig. ۳: (a)-(b) *Effective index* and *loss* variations versus *w* when *h*=۲۰۰nm, *t*=٥۰nm, and *w*=۳۰۰:۹۰۰nm with ٥۰nm steps, respectively.

For this mode at *w*=۷۰۰nm, the *loss* is as high as ۹,۹×۱۰$^5$ □□/□□ □□□ □□□□□□□□ □□□□□□□□□□ □□ □□□ □□□□□□ of ۹,۳۱×۱۰$^5$ dB/cm. AS$^{1st}$, AS$^{2nd}$, and S$^{1st}$ has a decremental loss response during this period. S$^{2nd}$ mode also has a gradual increase and saturates at ۶,۹×۱۰$^5$ at the end of the interval.

### ۳,۳ □□□□□□□□ □□□ □□ □□□□□ □□□□□□□□□□
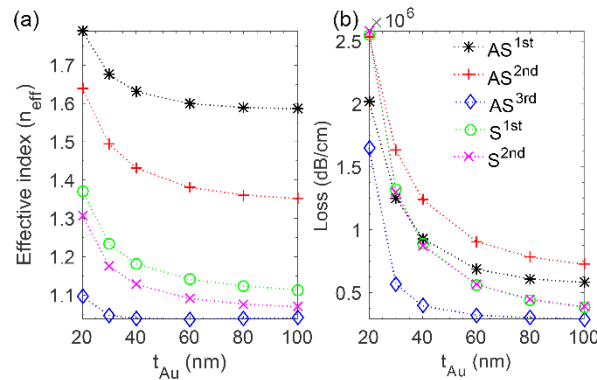


Fig. ٤: (a)-(b) *Effective index* and *loss* variations for *t*=۲۰:۱۰۰nm, *h*=۲۰۰nm, and *w*=٥۰۰nm.

In Fig. ٤(a)-(b), we have demonstrated the effect of the metal layer thickness *t* on the $n_{eff}$ and *loss* of the channel. At the frequency of ۳۶۰THz and constant values of *h*,*w*, and RI of the middle layer, we swept *t* from ۲۰ to ۱۰۰nm by ۱۰nm steps. It's noticeable that the amount of the $n_{eff}$ and *loss* has been decreased in all five modes over the variation interval of *t*. Based on the results AS$^{2nd}$ mode has

The ۲۸th Iranian Conference on Optics and Photonics (ICOP ۲۰۲۲)
The ۱۴th Iranian Conference on Photonics Engineering and Technology (ICPET ۲۰۲۲)
Shahid ChamranUniversity of Ahvaz, Khuzestan, Iran, Feb. ۱-۳, ۲۰۲۲.

the highest decrease of $n_{eff}$ by a value of ۰,۲۸۷. In contrast, the AS$^{۳rd}$ mode had the lowest decay by the value of ۰,۰۵ and remained approximately constant for the rest of the interval. Hence, the symmetric modes had the highest rate of decay of loss of around ۲,۱×۱۰٦ up to the end of the interval. The AS$^{۳rd}$ had the most rapid drop of loss for the interval of $t$ between ۲۰ and ۳۰nm.

### ۳,۴ ⬜⬜⬜⬜⬜⬜⬜⬜⬜ ⬜⬜ ⬜⬜⬜ ⬜⬜⬜⬜⬜⬜ ⬜⬜⬜⬜⬜⬜⬜⬜

In this simulation, we have changed the frequency $f$ of the excited modes from ۳۰۰ to ۴۴۰ THz (~ ۹۹۹ to ٦۸۱nm) with ۲۰THz steps. The graphs on Fig. ۵(⬜)–(⬜) ⬜⬜⬜⬜ ⬜⬜⬜⬜ ⬜⬜⬜ ⬜⬜⬜⬜⬜⬜⬜⬜⬜ ⬜⬜ ⬜⬜⬜ ⬜⬜⬜⬜⬜⬜⬜⬜⬜ leads to an increase in both $n_{eff}$ and *loss* in all modes.
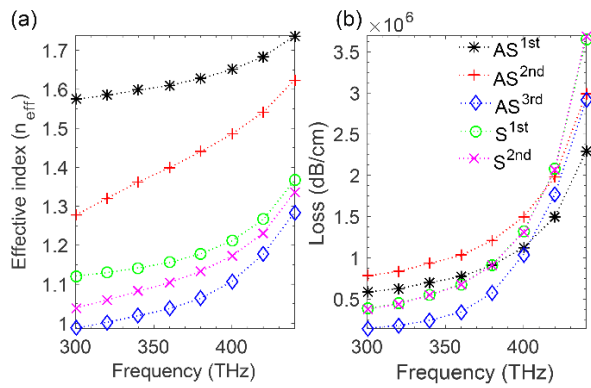


Fig. ۵: (a)-(b) *Effective index* and *loss* variations. $h=$۲۰۰, $t=$۵۰, and $w=$۵۰۰nm. $f=$۳۰۰:۴۴۰THz

According to Fig. ۵(a), the $n_{eff}$ of the AS$^{۲nd}$ mode has the highest rate of variation of about ۰,۳۴ and it has approximately a linear response in the given range of $f$. According to Fig. ۵(b), the S$^{۲nd}$ and S$^{۱st}$ modes show high sensitivity to frequency changes due to the highest variation of the *loss* parameter of about ۳,۳۱×۱۰٦ dB/cm. In contrast, the AS$^{۱st}$ mode shows the least changes in both $n_{eff}$ and loss.

### ۳,۵ ⬜⬜ ⬜⬜ ⬜⬜⬜ ⬜⬜⬜⬜⬜⬜⬜ ⬜⬜⬜⬜⬜

Fig. ٦(a) illustrates the variation of $n_{eff}$ when the refractive indices *RI* of sensing media changs. In this simulation, we have investigated the capability of the structure in sensing different target materials.

The *RIs* for the selected layer are ۱,۳۳, ۱,۴۵, ۱,۵۵, and ۱,٦۵ while all other parameters such as $h$, $t$, $w$, and $f$ remained constant.
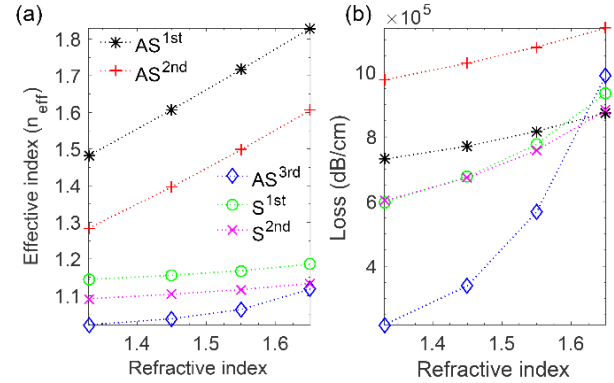


Fig. ٦: (a)-(b) *Effective index* and *loss* variations versus RI for $h=$۲۰۰nm, $t=$۵۰nm, $w=$۵۰۰nm.

It's noticeable that by increasing the *RI* of the middle layer, the $n_{eff}$ and *loss* increase (Fig. ٦(a)-(b)). The AS$^{۱st}$ and AS$^{۲nd}$ has the highest $n_{eff}$ variation of about ۰,۳۴۷۹ ⬜⬜⬜ ۰,۳۲۱۴ ⬜⬜⬜⬜⬜⬜⬜⬜⬜⬜⬜⬜⬜. ⬜⬜⬜⬜, ⬜⬜⬜ variations of these two modes are perfectly linear in both graphs. The loss graph also demonstrates that the AS$^{۳rd}$ has the highest *loss* variation of about ۷,۷۱۷×۱۰۵ dB/cm.

## ۴. Conclusion

According to the simulation results, for the given MIM structure, the $n_{eff}$ and *loss* strongly depend on the structure geometry, dielectric material, and injection mode frequency. By utilization of the proper mode profile and geometry optimization, a high sensitive Opto-sensor can be realized.

## References

[۱] V. G. Kravets, A. V. Kabashin, W. L. Barnes and A. N. Grigorenko, "Plasmonic Surface Lattice Resonances: A Review of Properties and Applications," *Chemical Reviews,* vol. ۱۱۸, no. ۱۲, pp. ۵۹۱۲-۵۹۵۱, ۲۰۱۸.

[۲] R. A. Alvarez-Puebla, J.-F. Li and X. Y. Ling, "Introduction to advances in plasmonics and its applications," *Nanoscale,* vol. ۱۳, no. ۱۲, pp. ۵۹۳۵-۵۹۳٦, ۲۰۲۱.

[۳] A. I. Fernández-Domínguez, F. J. García-Vidal and L. Martín-Moreno, "Unrelenting plasmons," *Nature Photonics,* vol. ۱۱, no. ۱, pp. ۸-۱۰, ۲۰۱۷.